AIP | Journal of Applied Physics

Surface-oxidation-induced phase separation in FeMn thin films

H. Lefakis, T. C. Huang, and P. Alexopoulos

Citation: Journal of Applied Physics **64**, 5667 (1988); doi: 10.1063/1.342268
View online: http://dx.doi.org/10.1063/1.342268
View Table of Contents: http://scitation.aip.org/content/aip/journal/jap/64/10?ver=pdfcov
Published by the AIP Publishing

Articles you may be interested in

Exchange biased FeNi/FeMn bilayers with coercivity and switching field enhanced by FeMn surface oxidation
AIP Advances **3**, 092104 (2013); 10.1063/1.4821105

A physical model of exchange bias in [Pd / Co] 5 / FeMn thin films with perpendicular anisotropy
J. Appl. Phys. **108**, 063924 (2010); 10.1063/1.3471803

"Villari reversal" in the exchange biased [Pd / Co] 5 / FeMn thin films with perpendicular anisotropy
Appl. Phys. Lett. **94**, 152512 (2009); 10.1063/1.3120556

Critical behavior in the reentrant phase of (P dFe)Mn
J. Appl. Phys. **67**, 5955 (1990); 10.1063/1.346026

Characterization of the surface oxidation and magnetic properties of MnFe thin films
J. Vac. Sci. Technol. A **6**, 918 (1988); 10.1116/1.575030

[This article is copyrighted as indicated in the article. Reuse of AIP content is subject to the terms at: http://scitation.aip.org/termsconditions. Downloaded to] IP: 35.8.11.3 On: Fri, 29 Jan 2016 16:37:56

Surface-oxidation-induced phase separation in FeMn thin films

H. Lefakis,[a] T. C. Huang, and P. Alexopoulos[a]
IBM Research Division, Almaden Research Center, 650 Harry Road, San Jose, California 95120-6099

Films of $Fe_{50}Mn_{50}$, 700 Å thick, were deposited on glass substrates by diode rf sputtering. Auger electron spectroscopy, and x-ray fluorescence analysis verified the film composition and x-ray diffraction determined the crystalline phase to be α-Mn(Fe), a complex bcc-like structure and a considerable deviation from that dictated by the equilibrium binary phase diagram. The films were annealed for 1 h at 260 °C and 10^{-7}, 10^{-5}, and 10^{-2} Torr. Auger depth profile analysis showed that (a) while no further oxidation (than that induced by ambient exposure) occurred during annealing at the lowest pressure, severe film oxidation took place at the highest pressure and (b) preferential surface oxidation of Mn resulted in a layered structure consisting of a surface Mn- and oxygen-rich layer followed by a region (deeper into the film) depleted in Mn and Fe enriched. The crystalline phases present were determined by x-ray diffraction analysis to be MnO (fcc) and α-Fe(Mn) (bcc). Magnetic measurements of the oxidized films revealed that they displayed in-plane isotropic ferromagnetic properties, with $4\pi M_s \sim 15$–18 kG for the most extensively oxidized films.

INTRODUCTION

FeMn alloy thin films have been of considerable interest to magnetic recording technology because of their potential application as a Barkhausen noise suppressant in magnetoresistive (MR) read heads.[1,2] The dependence of exchange-induced unidirectional anisotropy in permalloy/FeMn films on film thickness,[3] annealing temperature,[4,5] and some deposition parameters[4] has been examined, while a recent study has been made of the room-temperature surface oxidation of FeMn thin films.[6] In the present work, the effect of ambient pressure (between 10^{-7} and 10^{-2} Torr) during annealing (at 260 °C) on the structural and magnetic phase stability as well as the surface oxidation characteristics of rf-sputtered FeMn thin films has been examined by x-ray fluorescence and diffraction techniques, *B-H* loop testing, and Auger electron spectroscopy analysis.

MATERIALS AND EXPERIMENTAL PROCEDURES

The FeMn films were produced by a Perkin Elmer (Model 2400) rf diode sputtering system on 0.2-mm-thick glass-slide substrates. The base pressure was 1.3×10^{-5} Pa (10^{-7} Torr), the operating pressure 2.6 Pa (20 μm), and the deposition rate ~ 1.6 Å s^{-1}. The film thickness (~ 700 Å) was measured by stylus techniques and x-ray fluorescence. Annealing was performed in the presence of a magnetic field, in a high vacuum (HV) furnace, for the 10^{-7} and 10^{-5} Torr annealing and in a separate low vacuum (LV) furnace, for the 10^{-2} Torr annealing. The temperature (260 °C) was monitored and controlled to $\pm$ 1 and 3 °C in the HV and LV furnaces, respectively.

X-ray fluorescence and diffraction analyses were performed with a wavelength dispersive Rigaku spectrometer and a vertical θ-2θ scanning Norelco diffractometer employing Cu$K\alpha$ x-rays. Auger analyses were carried out with a PHI 600 Scanning Auger Microprobe. To avoid overlap among the Fe and Mn L_3MM transitions, the Fe-$L_3M_{45}M_{45}$ (~ 703 eV) and the Mn-$L_3M_{23}M_{23}$ (~ 542 eV) were monitored during Auger depth profiling. The contribution of the Mn-L_2MM to the principal O-KLL was not readily quantifiable, due to data scarcity, and was considered rather small to entail correction. Compositional profiles (in at. % concentration) were obtained from peak-to-peak Auger signals using elemental sensitivity factors[7] derived from standards prepared in the same sputter system and analyzed by x-ray fluorescence.

RESULTS AND DISCUSSION

The composition of the films before annealing, determined by x-ray fluorescence analysis, was found to be 50.7 at. % Fe and 49.3 at. % Mn. Auger depth profiles showed that the films were of uniform composition throughout (Fig. 1), containing only low levels of oxygen (part of the O signal is due to the Mn contribution), and no other detectable impurities. The native oxide formed by handling in air following deposition was Mn rich and relatively thick (~ 50 Å). X-ray diffraction analysis of these films [Fig. 2(a)] showed that their crystalline structure is α-Mn(Fe) (basically α-Mn, or A12 type), a complex cubic structure containing 58 atoms per unit cell, as compared to 2 atoms/unit cell of the simple bcc.[8] This structure is different from that dictated by the bulk equilibrium binary phase diagram[9] for the equal atomic ratio composition, an fcc-γ phase. Deviations from the equilibrium phase diagram are not uncommon for thin films and indeed one has been reported for this system though only for the primary α-Fe region (low Mn concentration).[10,11] The deviation of the presently observed phase is rather considerable (~ 18 at. %) and has not been pre-

[a] IBM Magnetic Recording Institute.

 0021-8979/88/225667-03$02.40 © 1988 American Institute of Physics

[This article is copyrighted as indicated in the article. Reuse of AIP content is subject to the terms at: http://scitation.aip.org/termsconditions. Downloaded to] IP: 35.8.11.3 On: Fri, 29 Jan 2016 16:37:56

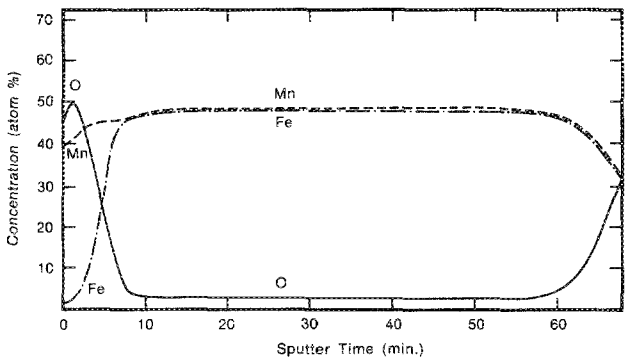

FIG. 1. Auger depth profile of a 700-Å-thick film of $Fe_{50}Mn_{50}$ rf-sputter deposited onto an unheated glass substrate.

viously reported, although incidental mention has been made of the importance of the substrate[1,3,6] in the formation of the preferred, equilibrium phase (γ). Since α-Mn is antiferromagnetic at low temperatures ($T_N \sim 100$ K)[12] no magnetic response was detected by ambient temperature *B-H* loop testing of these films [Fig. 3(a)].

Annealing these films at 260 °C and 10^{-7} Torr vacuum for 1 h did not affect them in any detectable way. Annealing however at higher pressures produced some noticeable changes. After 1 h at 10^{-5} Torr, the films formed a thick surface oxide, ~100–150 Å thick, which is Mn rich (Fig. 4, region I). Almost no Fe could be detected at the surface and within the oxide the Fe concentration was very low (~1%–2%). Adjacent to the oxide layer there exists a region of roughly equal thickness, which is Fe rich and Mn depleted as compared to the initial composition of the film (Fig. 4, region II). Between this region (II) and the substrate (Fig. 4, region III), the composition is identical to that of the films

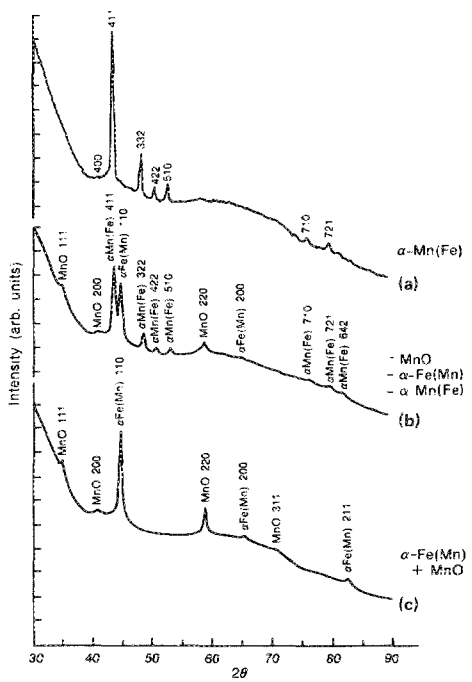

FIG. 2. X-ray diffraction spectra of $Fe_{50}Mn_{50}$ films: (a) after deposition (same specimen as described in Fig. 1), (b) after annealing at 10^{-5} Torr (same specimen as described in Fig. 4), and (c) after annealing at 10^{-2} Torr (same specimen as described in Fig. 5).

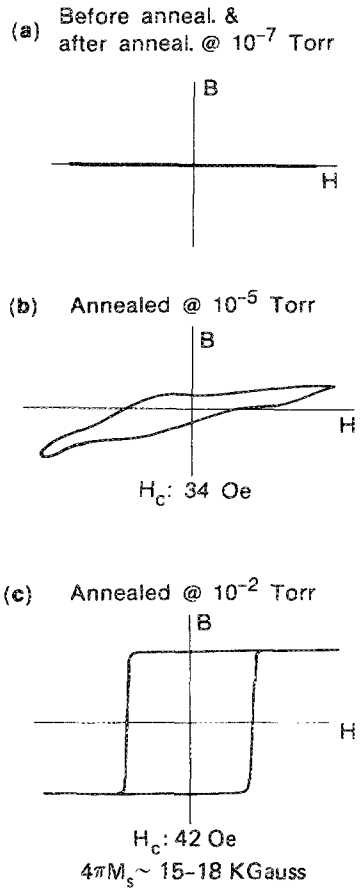

FIG. 3. *B-H* loop results of a FeMn specimen (prepared as described in Fig. 1): (a) before annealing and after annealing at 10^{-7} torr, (b) after annealing at 10^{-5} Torr, and (c) after annealing at 10^{-2} Torr. All annealing was performed at 260 °C for 1 h.

before annealing (compare Figs. 4 and 1). The apparent mass balance between regions I and II show that the preferential oxidation of Mn at the surface has driven Mn migration from region II, leaving it Fe rich.

X-ray diffraction analysis of this annealed specimen [Fig. 2(b)] allowed structural identification of the three regions. The top oxide (region I, Fig. 4) is MnO, in agreement with the Auger data and the recently reported XPS results of FeMn oxidation at room temperature.[6] Regions II and III were found to be α-Fe(Mn) and α-Mn(Fe), respectively. [In order to avoid confusion about FeMn alloy phases, the notation α-Fe(Mn) and α-Mn(Fe) has been used throughout this paper to refer to α-Fe and α-Mn structures, respectively.] For the Fe/Mn composition of this region (II, Fig. 4) this phase too is not implied by the equilibrium phase

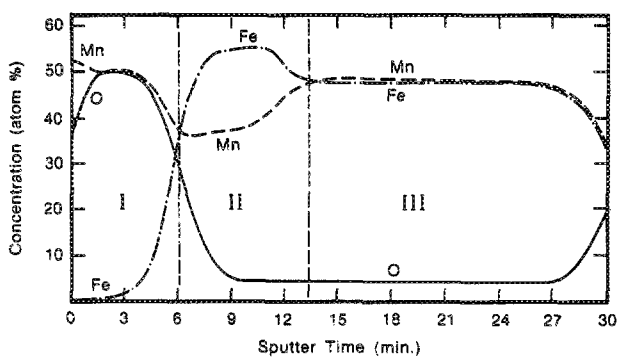

FIG. 4. Auger depth profile of a FeMn specimen (prepared as described in Fig. 1) after annealing for 1 h at 260 °C and 10^{-5} Torr.

[This article is copyrighted as indicated in the article. Reuse of AIP content is subject to the terms at: http://scitation.aip.org/termsconditions. Downloaded to] IP: 35.8.11.3 On: Fri, 29 Jan 2016 16:37:56

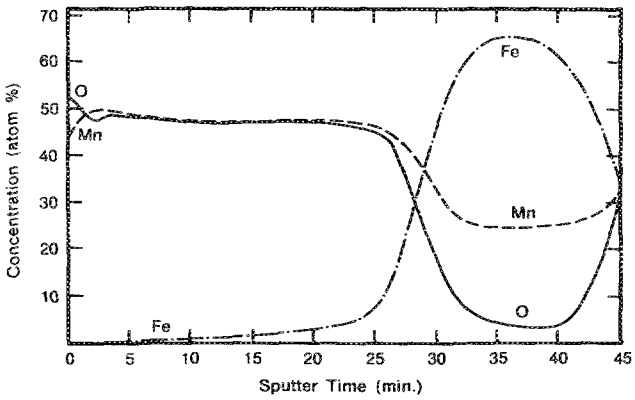

FIG. 5. Auger depth profile of a FeMn specimen (prepared as described in Fig. 1) after annealing for 1 h at 260 °C and 10^{-2} Torr.

diagram. In addition, though its composition is close to the upper boundary of the two-phase field observed in metastable FeMn alloys ($\sim$35 at. % Mn),[11(b)] no γ-FeMn was detected. The metastable α-Fe(Mn) observed here therefore represents a larger departure from the equilibrium phase (<3 at. % Mn)[9] than previously reported ($\sim$20 at. % Mn).[10,11]

Annealing at a higher pressure (10^{-2} Torr) caused a much more severe oxidation, extending through more than half of the film thickness (Fig. 5). As with the samples annealed at 10^{-5} Torr (Fig. 4), the top oxide layer seems to be of the MnO type with no or little Fe present. The preferential oxidation of Mn at the surface depletes the remainder of the film of Mn and enriches it with Fe. The oxidation in this case has been sufficiently severe to affect the entire film and has left no layer of the original alloy intact, as inferred by the composition profile. In agreeement with these observations, x-ray data [Fig. 2(c)] have identified the presence of only MnO and α-Fe(Mn) in these heavily oxidized films. As with the samples annealed at 10^{-5} Torr, no γ-FeMn was detected although the Fe/Mn concentration ratio in the unoxidized region (Fig. 5) implied its presence.[9,11(b)]

The metastable α-Fe(Mn) phase has been reported to be ferromagnetic at room temperature, up to a Mn concentration of $\sim$20 at. % at which point a bcc-to-fcc transition was observed.[10] *B-H* loop measurements of our samples [containing metastable α-Fe(MN) phases of even higher Mn concentration] have also shown ferromagnetism. The sample annealed at 10^{-5} Torr [Fig. 3(b)] showed the appearance of magnetic hysteresis while the sample annealed at 10^{-2} Torr [Fig. 3(c)] displayed well-defined in-plane isotropic ferromagnetic properties. Using *B-H* loop data and thickness estimates from Auger profiles, for this phase region, the saturation magnetization ($4\pi M_s$) for this metastable α-Fe(Mn) phase was estimated to be $\sim$15–18 kG. This range reflects the $\sim$20% inaccuracy of the thickness (of the phase region) but is consistently lower than the handbook value for pure Fe (21.6 kG).[12] FMR measurements performed on these films were consistent with these saturation magnetization values.

It is interesting to note that the ferromagnetic character of a Fe-based phase, seems to be more closely related to the crystalline structure of that phase than to its composition. The metastable bcc-α-Fe(Mn) phase of this work does remain ferromagnetic despite its high average concentration of Mn ($\sim$25–35 at. %). This observation is consistent with results from Mössbauer effect measurements on FeMn that the atomic moment and the internal field of Fe atoms are not very sensitive to the Mn atom concentration in bcc $Fe_{1-x}Mn_x$ ($x = 0.04$–0.13) alloys.[14]

Another interesting observation in this work is the fact that one metastable phase [the bcc-α-Mn(Fe), of the Mn terminal solution] transforms to another metastable phase [the bcc-α-Fe(Mn), of the Fe terminal solution], instead of the intermediary equilibrium phase (fcc-γ-FeMn), as oxidation-induced Fe/Mn composition changes occur during HV and LV annealing. Since this phase transformation is driven by the preferential oxidation of Mn at the surface, the degree of its occurrence is controlled by the MnO nucleation and growth characteristics for this particular system; i.e., atomic diffusion of Mn, O, and possibly Fe through, and kinetics of the growing oxide.

[1] R. D. Hempstead, S. Krongelb, and D. A. Thompson, IEEE Trans. Magn. **MAG-14**, 521 (1978).
[2] C. Tsang, J. Appl. Phys. **55**, 2226 (1984).
[3] C. Tsang, N. Heiman, and K. Lee, J. Appl. Phys. **52**, 2471 (1981).
[4] C. Tsang and K. Lee, J. Appl. Phys. **53**, 605 (1982).
[5] W. C. Cain, W. H. Meiklejohn, and M. H. Kryder, J. Appl. Phys. **61**, 4170 (1987).
[6] S. L. Cohen, M. A. Russak, J. M. Baker, T. R. McGuire, G. J. Scilla, and S. M. Rossnagel, J. Vac. Sci. Technol. (in press).
[7] L. E. Davis, N. C. MacDonald, P. W. Palmberg, G. E. Riach, and R. E. Weber, *Handbook of Auger Electron Spectroscopy* (Physical Electronics, Eden Prairie, MN, 1976).
[8] R. W. G. Wyckoff, *Crystal Structures*, 2nd ed. (Interscience, New York, 1963), Vol. 1.
[9] M. Hansen and K. Anderko, *Constitution of Binary Alloys* (McGraw-Hill, New York, 1958).
[10] K. Sumiyama, M. Kadono, and Y. Nakamura, Trans. J. Int. Magn. **22**, 686 (1981).
[11] (a) K. Sumiyama and Y. Nakamura, Trans. J. Int. Magn. **23**, 595 (1982); (b) J. Magn. Magn. Mater. **35**, 219 (1983).
[12] (a) B. D. Cullity, *Introduction to Magnetic Materials* (Addison-Wesley, Reading, MA, 1972); (b) T. F. Connolly and E. D. Copenhaver, *Bibliography of Magnetic Materials Solid State Physics Literature Guides, Vol.5* (IFI/Plenum, New York, 1972).
[13] S. G. Kang, H. Onodera, H. Yamamoto, and H. Watanabe, J. Phys. Soc. Jpn. **36**, 975 (1974).

[This article is copyrighted as indicated in the article. Reuse of AIP content is subject to the terms at: http://scitation.aip.org/termsconditions. Downloaded to] IP: 35.8.11.3 On: Fri, 29 Jan 2016 16:37:56